Appl. Phys. B 68, 975–982 (1999) / DOI 10.1007/s003409900033

Applied Physics B
Lasers
and Optics

Interaction of two-dimensional spatial incoherent solitons in photorefractive medium

W. Królikowski[1], B. Luther-Davies[1], C. Denz[2], J. Petter[2], C. Weilnau[2], A. Stepken[2], M. Belić[3]

[1] Australian Photonics Cooperative Research Centre, Laser Physics Centre, Australian National University, Canberra ACT 0200, Australia
(Fax: +61-26/249-0029, E-mail: wzk111@rsphy1.anu.edu.au)
[2] Institute of Applied Physics, Technische Hochschule Darmstadt, 64289 Darmstadt, Germany
[3] Institute of Physics, P.O. Box 57, 11001 Belgrade, Yugoslavia

Received: 16 November 1998/Revised version: 12 February 1999/Published online: 12 April 1999

Abstract. We present a review of our recent theoretical and experimental results on the interaction of incoherent two-dimensional solitary beams in PR SBN crystals. We show that the inherent anisotropy of PR nonlinearity strongly affects the interaction between solitons. Theoretical and experimental results reveal that solitons interacting in a plane perpendicular to the direction of external biasing field always attract, whereas those colliding in a plane of the field exhibit anomalous behaviour. They may experience both attractive and repulsive forces, depending on their mutual separation. We also show that this anisotropy results in the complicated topology of soliton trajectories, featuring periodic collisions, prolonged mutual spiraling and collapse, depending on the initial conditions.

PACS: 42.65.Tg; 03.40.Kf; 42.65.Hw

Photorefractive (PR) crystals biased with a dc electric field have been shown to support formation and propagation of the so-called screening spatial solitons at very moderate laser powers. This is in contrast to the experimental realization of spatial solitons in a traditional Kerr-type material with electronic-type nonlinearity, which requires rather high light intensities.

As an optical beam propagates in a PR crystal, the distribution of photoexcited charges induces a space-charge electric field which screens out the externally applied field. The effective spatially varying electric field modulates the refractive index of the medium in such a way that the beam becomes self-trapped by a locally increased index of refraction and may propagate as a spatial soliton [1–7]. The ease of formation and manipulation using very low laser power (microwatts), as well as their stability and robustness makes the screening solitons very attractive for practical applications. Because of their accessibility, screening solitons have also become a very useful tool in experimental verification of many theoretical predictions concerning general soliton theory, in particular soliton collisions.

Dedicated to Prof. Dr. Eckard Krätzig on the occassion of his 60th birthday.

The spatial solitons are ideally suited for application in all-optical beam switching and manipulation. This concept is based on the ability to implement logic operations by allowing solitons to collide in a nonlinear medium [8, 9], as well as on the possibility of soliton-induced waveguides being used to guide and switch additional beams [10, 11]. Efficient implementation of this concept requires a detailed understanding of the nature of soliton interaction. Two types of soliton interaction (collision) can be realized in a PR medium. If both solitons have exactly the same frequency, then their interaction is coherent and the outcome of the collision strongly depends on the relative phase of solitons. This type of interaction was demonstrated in recent experiments with screening solitons, where soliton fusion, energy exchange [12–14] as well as "soliton birth" [15] and soliton annihilation [16] have been observed. By introducing a frequency shift into one of the soliton-forming beams one can realize an incoherent interaction. PR medium is slow, and for sufficiently large frequency detuning the refractive index change induced by the interacting beams will be the function of the sum of their intensities, regardless of their relative phases. Since the phase control of solitons can be difficult to achieve, the incoherent interaction is actually more interesting as far as the practical applications are concerned. Incoherent soliton interaction leading to the soliton fusion and spiraling has been reported in [17–19].

In this work we present a review of our recent experimental and theoretical studies concerning the interaction and collision of incoherent PR screening solitons. In order to precisely determine trajectories of interacting solitons one would have to visualise beams as they propagate inside the photorefractive crystal. However the imaging of solitons inside the crystal is not possible. The only quantity that can be recorded in experiments is the position of interacting beams at the input and output of the crystal. However, such observation is insufficient to describe topology of soliton trajectories. For this reason we analyze the outcome of the soliton interaction by employing not only experimental observations but also numerical simulations which allow for the probing of the details within the crystal.

The paper is organized as follows. Section 1 describes the basic experimental configuration used in our studies.

In Sect. 2 we present a theoretical model of formation and propagation of screening solitons in PR media. Section 3 is devoted to the soliton formation process. In Sect. 4 we discuss the interaction of incoherent solitons. Finally, Sect. 5 concludes the paper.

1 Experimental configuration

All soliton interaction scenarios are investigated experimentally in a configuration shown schematically in Fig. 1. The sample of PR strontium barium niobate crystal was biased with a high-voltage dc field of about 2–3 kV applied along its polar *c* axis. Two circular beams derived from a frequency-doubled Nd:YAG laser ($\lambda = 532$ nm) were directed by a system of mirrors and beam splitters on the entrance face of the crystal. At these locations the beams had Gaussian diameters of 10 μm, and were polarized along the *x* axis (which coincides with the polar axis of the crystal), to make use of the r_{33} electrooptic coefficient. In the experimens we used SBN crystal doped with Cerium (0.002% by weight). It measured $13.5 \times 5 \times 5$ mm ($\hat{a} \times \hat{b} \times \hat{c}$). The PR nonlinearity has a saturable character. Thus, the parameters of screening solitons are determined by the degree of saturation, which is defined as the ratio of the soliton peak intensity to the intensity of the background illumination. To control the degree of saturation we illuminated crystals by a wide beam derived from a white-light source [20]. In all our experiments the power of each input beam did not exceed a few microwatts and the power of background illumination was set to such level that the degree of saturation was estimated to be of the order of unity for all beams. One of the input beams was reflected from a mirror mounted on a piezo-electric transducer. Driving this transducer by an ac signal of several kHz made the beams effectively incoherent, because of the slow response of the PR medium, hence allowing for incoherent interaction. The relative angle of the interacting beams could be precisely adjusted by external mirrors. In most experiments it did not exceed 1°. The input and output light intensity distributions were recorded with a CCD camera and stored in the computer.

2 Theoretical model

The two-dimensional analysis of the formation, stability and nonlinear evolution of the (2+1)D soliton-type structures in PR media is crucial for a complete understanding of collisional properties of solitons. This is because of special features of the PR nonlinearity. Photorefractive material responds to the presence of the optical field $E(\boldsymbol{r})$ by a nonlinear change in the refrative index Δn that is both anisotropic and nonlocal function of the light intensity. The anisotropy does not allow radially symmetric soliton solutions, thereby requiring an explicit treatment of both transverse coordinates [21]. The nonlocality is another feature of the PR response that makes it significantly different from the typical nonlinear optical media, where the nonlinear refractive index change is a local function of the light intensity. This local response, in the simplest case of an ideal Kerr-type medium $\Delta n \propto |E|^2$, results in the canonical nonlinear Schrödinger equation for the amplitude of light propagating in the medium. A more realistic model results in the appearance of higher order nonlinearities which are an indication of the saturable (but still local) character of the nonlinearity [22]. In contrast, in PR media the change in the refractive index is proportional to the amplitude of the static electric field induced by the optical beam. Finding the material response therefore requires solving an elliptical-type equation for the electrostatic potential, with a source term due to the light-induced generation of mobile carriers [23, 24].

To describe the formation and interaction of screening solitons in PR media we use the model based on the Kukhtarev material equations and the paraxial approximation to the propagation of optical beams [25]. We assume that the optical field consists of two scalar monochromatic beams

$$E(\boldsymbol{r}, t) = \left[A(\boldsymbol{r}, t)\exp(\mathrm{i}\boldsymbol{k_1}\cdot\boldsymbol{r}) + B(\boldsymbol{r}, t)\exp(-\mathrm{i}\Omega t)\exp(\mathrm{i}\boldsymbol{k_2}\cdot\boldsymbol{r})\right] \times \exp(-\mathrm{i}\omega t) + \text{c.c.}\,, \tag{1}$$

separated by the frequency shift Ω. If this frequency difference is such that $\Omega\tau \gg 1$, where τ is the characteristic response time of the nonlinearity, then the nonlinear medium is not able to follow fast changes of the relative phase between beams and the beams propagate and interact as if they were temporally incoherent. The beam propagation along the *z* axis of a PR crystal with an externally applied electric field along the *x* axis is described by the following equations [6, 26]

$$\left[\frac{\partial}{\partial z} + \boldsymbol{\theta_1}\cdot\nabla - \frac{\mathrm{i}}{2}\nabla^2\right] A(\boldsymbol{r}) = \mathrm{i}\gamma\left(\frac{\partial\varphi}{\partial x} - E_0\right) A(\boldsymbol{r})\,, \tag{2a}$$

$$\left[\frac{\partial}{\partial z} + \boldsymbol{\theta_2}\cdot\nabla - \frac{\mathrm{i}}{2}\nabla^2\right] B(\boldsymbol{r}) = \mathrm{i}\gamma\left(\frac{\partial\varphi}{\partial x} - E_0\right) B(\boldsymbol{r})\,, \tag{2b}$$

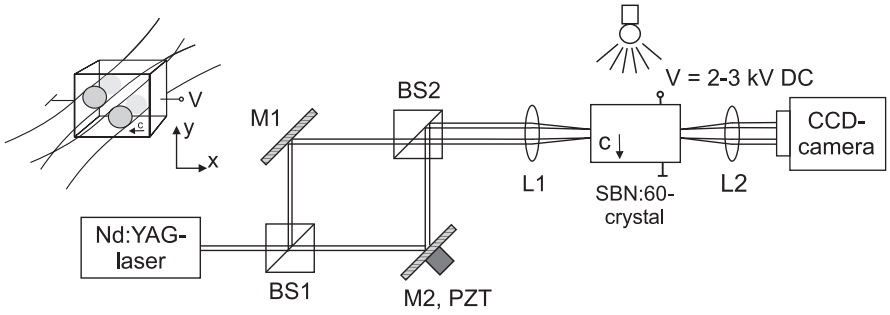

Fig. 1. Schematic configuration of soliton interaction. BS, beam splitters; M_1, M_2, mirrors; L_1, L_2, lenses; PZT, piezoelectric transducer; *V*, voltage

$$\tau\frac{\partial}{\partial t}(\nabla^2\varphi)+\nabla^2\varphi+\nabla\varphi\cdot\nabla\ln(1+I)=E_0\frac{\partial}{\partial x}\ln(1+I)$$
$$+\frac{k_{\mathrm{B}}T}{e}\left\{\nabla^2\ln(1+I)+[\nabla\ln(1+I)]^2\right\}\,, \qquad (2c)$$

where $\boldsymbol{\theta_1}$ and $\boldsymbol{\theta_2}$ specify the initial directions of both beams, ∇ is the transverse gradient, and $\gamma = k^2n^4x_0^2r_{\mathrm{eff}}$ is the medium–light coupling constant. Here $k=|\boldsymbol{k}_1|=|\boldsymbol{k}_2|$ is the wave number of light, n is the index of refraction, x_0 is the typical beam spot-size, and r_{eff} is the effective element of the electro-optic tensor. The transverse coordinates x and y are scaled by x_0 and the propagation coordinate z is scaled by the diffraction length $L_{\mathrm{D}}=knx_0^2$. φ is the electrostatic potential induced by the light, with the boundary conditions $\nabla\varphi(\boldsymbol{r}\to\infty)\to 0$ and E_0 is the external field. The normalized intensity $I=|A|^2+|B|^2$ is measured in units of the saturation intensity. The last term on the right-hand side of (2c) is due to the diffusion of charges in the crystal. It causes beams to bend. The set of equations (2) is integrated numerically for a range of initial conditions. All material parameters correspond to typical values encountered in SBN crystal [27]. In all simulations the input beams are assumed to be Gaussian of sufficient intensity and shape to yield solitons.

3 Soliton formation

As we have already mentioned, the screening solitons are formed through the refractive index change induced via Pockels effect by the spatially modulated electric field. The modulation of the static field is achieved by screening the biasing dc field through excitation of electric charge carriers. Since the screening involves the transport of charge carriers, the time scale of the process equals that of the typical PR effect – typically from ms to s, depending on the particular material and light intensity [28]. The dynamics of soliton formation has been studied numerically in [6]. It has been shown that the steady state is reached after several stages of focusing and defocusing. In Fig. 2 we demonstrate the formation of a single 2-dimensional soliton. The graphs show intensity distribution at the exit face of the crystal at different times. The sequence starts at approximately 0.65 s after the elctric field was turned on. The time step between subsequent frames (#1−#11) is 0.5 s. The last graph (frame #12) illustrates the intensity distribution in the steady state. Initially the process exhibits strong focusing predominantly along the axis of the applied electric field. However, as time progresses the focusing along the other transverse dimension becomes pronounced as well. One can clearly observe the temporal evolution of the beam size. It significantly decreases initially, then slightly increases, decreases again and finally, after a few seconds, the steady state is reached, when the beam is focused into a slightly elliptical spot. It is also apparent from Fig. 2 that during the transient phase the beam moves along the direction of the applied field, so that in the steady state its position differs considerably from the initial position. The reason for this lateral shift of the beam lies in the nonlocal contribution to the refractive index change. It is due to diffusion of photoexcited charges and leads to an asymmetric refractive index change which, in turn, causes the beam to bend as it propagates through the crystal. This so-called self-bending effect [29, 30] depends on the spatial scale of the beam and can be as high as tens of μm over the propagation distance of few mm.

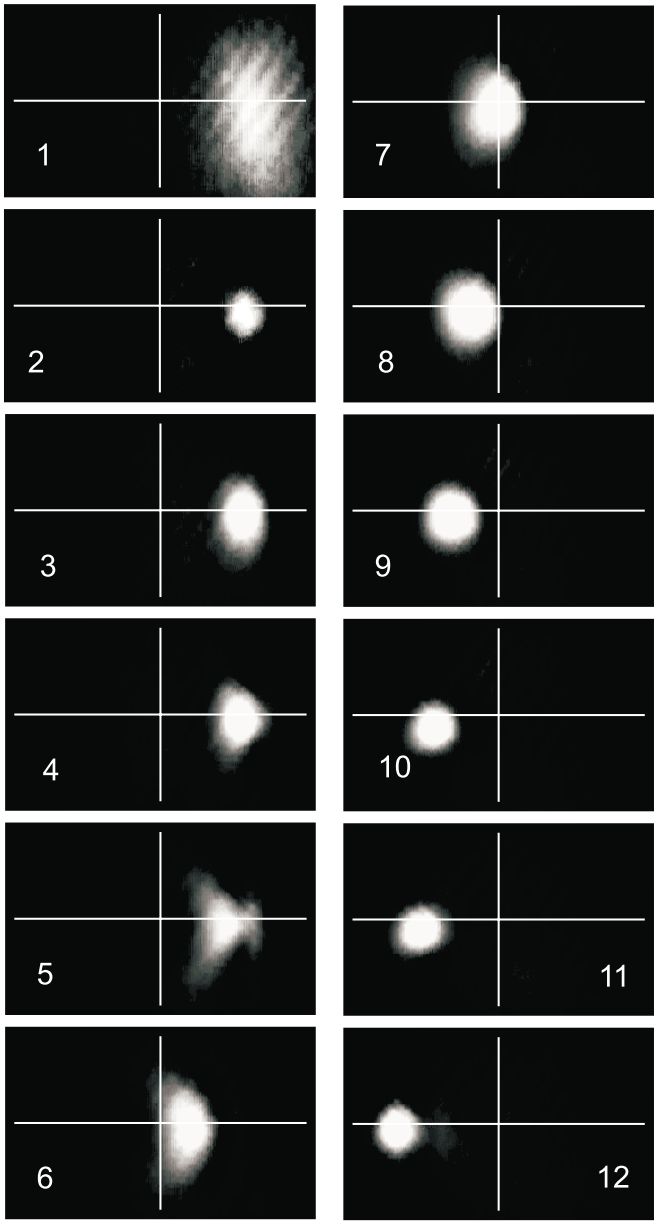

Fig. 2. Temporal evolution of the screening soliton. The time step between frames #1–#11 is 0.5 s; frame #12 illustrates the steady state

4 Interaction of incoherent solitons

In a typical isotropic self-focusing medium mutually incoherent solitons always attract each other. This is because the total light intensity always increases in the region where the beams overlap. This leads to an increase in the refractive index and subsequent attraction of the solitons. Several recent works have studied incoherent soliton interactions in PR media, demonstrating effects generic for the solitons of saturable nonlinear media [17]. On the other hand, we have shown recently that it is possible to achieve both attractive and repulsive interaction between mutually incoherent solitons in

PR medium [26, 31]. This anomalous situation is caused by the particular anisotropic and nonlocal structure of the PR nonlinearity and results in both attraction and repulsion of parallel beams depending on their relative spatial separation. Using numerical simulations and experimental observations we will show below that the PR anisotropy affects interaction of spatial solitons, leading to a complex topology of soliton trajectories.

4.1 Anisotropic nonlinear response

It has been pointed out by Zozulya and Anderson [6] that the nonlinear response of a PR crystal to the single optical beam is strongly anisotropic. First, the optical lens induced by the beam is astigmatic [32, 33], which results in typically elliptical intensity profile of the steady-state solitons. Second, and more important as far as the soliton interaction is concerned, the asymptotic behaviour of the light-induced refractive index change is drastically different along the two principal transverse directions. Along the *y* axis, i.e. in the direction perpendicular to the direction of the applied field, refractive index shows behaviour analogous to that seen for a Kerr-type nonlinearity. It reaches peak value in the centre of the beam and then monotonically decays to zero for large *y*. The situation is different along the direction of the applied biasing field (*x* axis). Away from the centre of the beam the refractive index first decreases, then changes the sign and monotonically approaches zero for large *y*. Sufficiently far from the centre of the beam the refractive index actually *increases* with light intensity, indicating self-defocusing. Such substantially different asymptotics lead to nonstandard interaction of two nearby solitons. In order to determine the detailed nature of this interaction one has to consider the refractive index change induced by two optical beams. In Fig. 3 we show the contour plots and profiles of the nonlinear index change in a thin slab of the PR crystal illuminated by two Gaussian beams. In the case depicted in Fig. 3a both beams are located along the *y* axis. For this orientation the refractive index change always *increases* in the region between beams, which indicates their attraction. This is a behaviour typical of self-focusing Kerr-type nonlinear media. For beams located along the direction of applied field the refractive index change depends on their separation. For closely placed beams (Fig. 3b) the index increases in the overlapping region and the beams attract. On the other hand, for large separation (Fig. 3c) the refractive index actually *decreases* in the overlapping region, which results in the repulsion of beams.

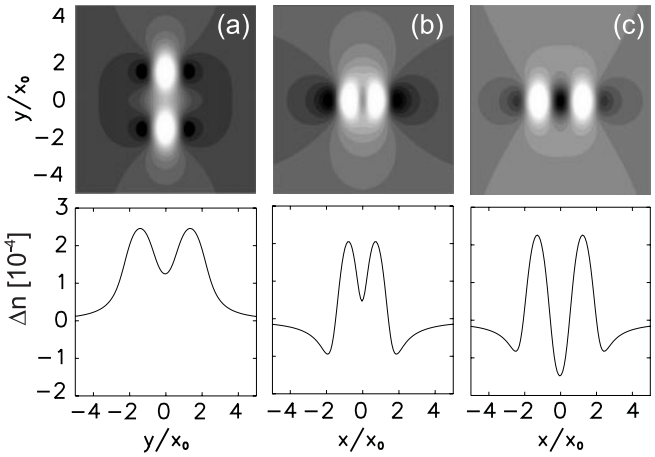

Fig. 3a–c. Nonlinear refractive index induced by two Gaussian beams in a thin slab of biased PR crystal. **a** Beams located along *y* axis. **b** Beams located along *x* axis, close separation. **c** Beams located along *x* axis, large separation

4.2 Normal interaction

As we have pointed out above, for incoherent solitons propagating in the plane perpendicular to the direction of the applied electric field, the nonlinear response of the medium is analogous to that of Kerr-like nonlinearity. This means that solitons always attract, independent of their separation. It is well known that attraction of solitons may result in the nontrivial character of their trajectories [34]. In particular, beams propagating in the same plane may form a bound state, with their trajectories periodically intersecting. It turns out that PR solitons display similar behaviour. We illustrate this in Fig. 4, where the numerically simulated interaction of initially parallel solitons propagating in the plane perpendicular to the

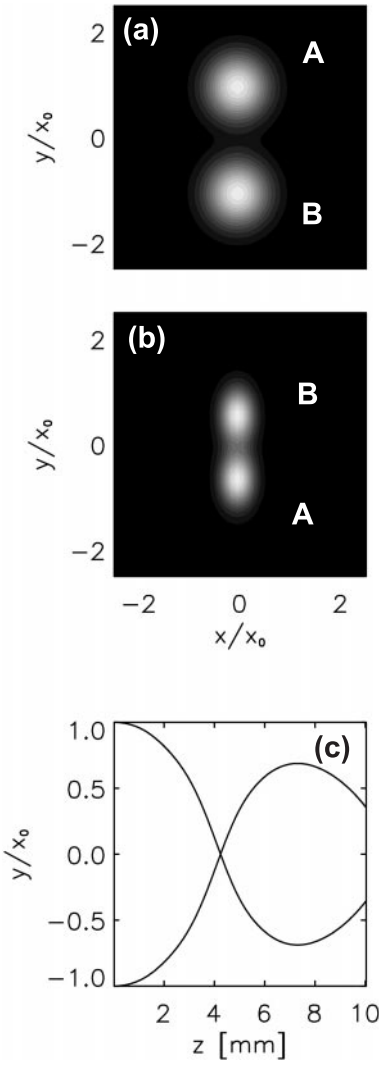

Fig. 4a–c. Numerical simulation of the interaction of solitons propagating in the plane perpendicular to the direction of the biasing field. **a** Input intensity distribution. **b** Output intensities. **c** Soliton trajectories

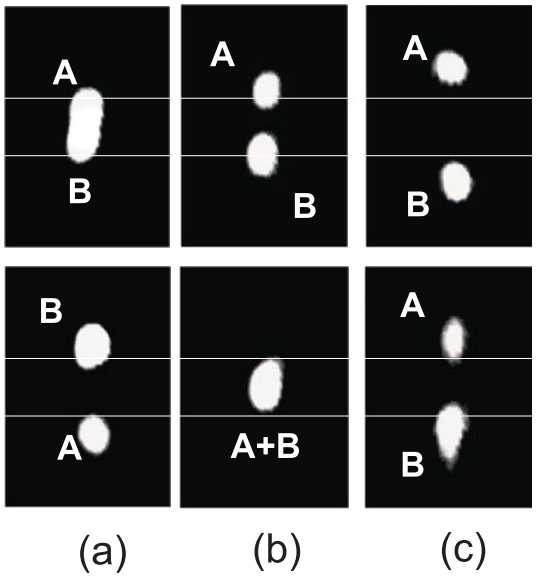

Fig. 5a–c. Experimental observation of attraction of incoherent solitons propagating in the *y* plane, for initial separation of 15 μm (**a**), 30 μm (**b**), and 50 μm (**c**)

direction of the applied field is shown. In Fig. 4a,b we show the input and output intensity distribution, respectively. For the chosen separation of the beams the attractive force leads to the interchange of beam positions. In the graph Fig. 4c we plot the calculated trajectories of both beams. Again, the attraction is clearly visible. It leads to the periodic collision of solitons. However, unlike the Kerr medium, where the soliton collisions are elastic [35], here the nonlinearity is of saturable character and collisions are inelastic. For this reason the amplitude of the mutual oscillation is damped and the solitons would eventually fuse. This is the generic behaviour of solitons in a saturable nonlinear media [36–38], colliding at a very small angle.

In Fig. 5 we demonstrate experimentally recorded strong attraction of screening solitons launched in the plane perpendicular to the direction of biasing field. In the first row we show the images of noninteracting solitons. These graphs were obtained by superimposing pictures corresponding to the individual propagation of solitons. The results of soliton interaction are displayed in the second row of this figure. For small separation of beams (15 μm – Fig. 5a) the strong attractive force causes the trajectories of both solitons to intersect. When the initial separation is increased to 30 μm (Fig. 5b) the attraction is weakened and it takes much longer distance for the solitons to collide. In this particular case solitons collide very close to the output face of the crystal, so that the output intensity exhibits a single peak structure. For larger initial separation (50 μm, Fig. 5c), a significantly weaker attraction results in a decreased separation at the exit face of the crystal.

4.3 Anomalous interaction

For solitons separated along the direction of applied field the outcome of the interaction depends on the separation distance. We study this effect by numerically integrating the propagation equations (2). Results are shown in Fig. 6. The first and second rows contain images of the input and output

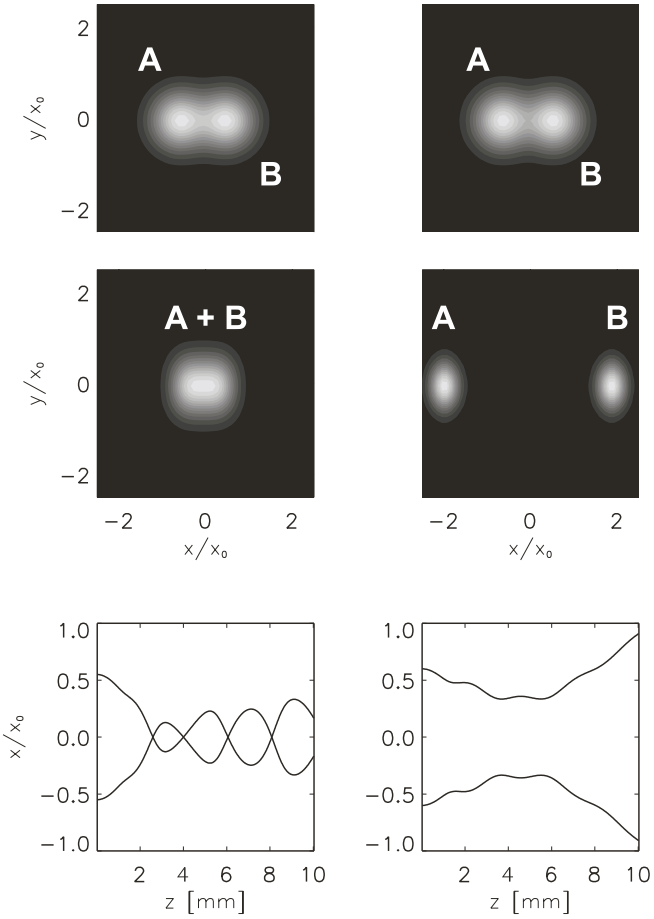

Fig. 6. Numerical simulations of the interaction of solitons propagating in the *y* plane. *Top row*: input intensity distribution; *middle row*: solitons at the exit face of the cryst; *bottom row*: soliton trajectories

intensity distributions, respectively. In the third row the soliton trajectories are shown. The first column corresponds to the closely spaced beams. For this separation the beams attract strongly, oscillating about the *z* axis and, as further simulations indicate, eventually coalescing into a single beam. An essentially different behaviour can be seen when the initial separation is increased (second column). Initially the beams overlap and refractive index between them slighty increases, leading to weak attraction. As soon as the solitons are formed, though, the repulsive interaction due to long defocusing tails in the refractive index distribution becomes evident. The separation between the solitons increases with propagation distance indicating mutual repulsion. In Fig. 7 we show more complex dynamics of the interacting solitons which are initially separated along both *x* and *y* axes. This time the propagation of initially parallel beams results in repulsion and a counterclockwise spiraling motion about the centre of the two beams.

Experimental results confirming the above numerical predictions are presented in Fig. 8, where we show input and output light intensity distributions for various initial separations of the beams. The first row of Fig. 8 shows the output intensity distribution for noninteracting solitons. These images were obtained by allowing each beam to propagate separately in the crystal and superimposing the resulting images. The second row contains the images of interacting solitons.

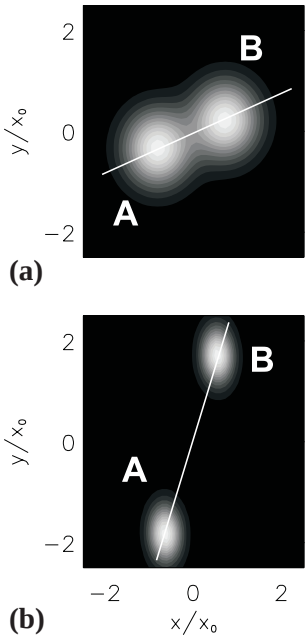

Fig. 7a,b. Numerical simulation of the mutual rotation of initially parallel solitons due to the anisotropy of PR nonlinearity. **a** Input beams. **b** Output beams (rotation due to interaction)

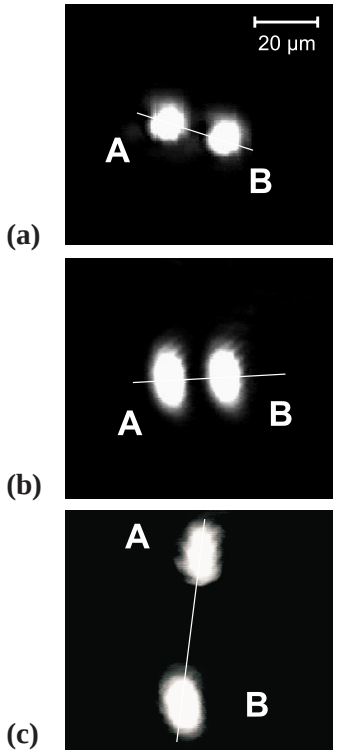

Fig. 9a–c. Experimentally observed soliton rotation due to the anisotropy of the PR nonlinerity. **a** Input beams. **b** Noninteracting solitons. **c** Rotation due to interaction

They were recorded when both beams were simultaneously present in the crystal. In the case of closely spaced solitons ($\approx 20\,\mu$m, Fig. 8a) the interaction is strongly attractive and the beams fuse, emerging from the crystal as a single solitary beam. This behaviour is essentially the same as that found for strongly overlapping solitons in a saturable Kerr-type nonlinearity. The situation changes dramatically when the initial separation between beams is increased to 40 μm, as shown in Fig. 8b. This time both input beams evolve into separate solitary waves as their separation increases, indicating mutual repulsion. Similar behaviour (with weaker repulsion) is observed for even larger separation (60 μm, Fig. 8c). Finally, for the input beams separated along both *x* and *y* axes, clear rotation of solitons is observed, as shown in Fig. 9. As the solitons interact, they not only increase their separation distance but also experience 80° spiraling about the centre of the beams. It should be emphasized that the spiraling motion is due to the anisotropy of the potential created by the two beams and occurs even though they are launched without any tangential velocity.

4.4 Interaction of skewed solitons

Some time ago it was predicted [34] that the incoherent spatial solitons in a self-focusing medium should spiral around each other if their mutual attraction can counterbalance the divergence of trajectories. A report on the experimental observation of this effect in a PR crystal has been published recently [18]. Mutual rotation for up to 540° over the propagation distance of 13 mm has been reported. For the spiraling to occur it is necessary to have attractive interaction between

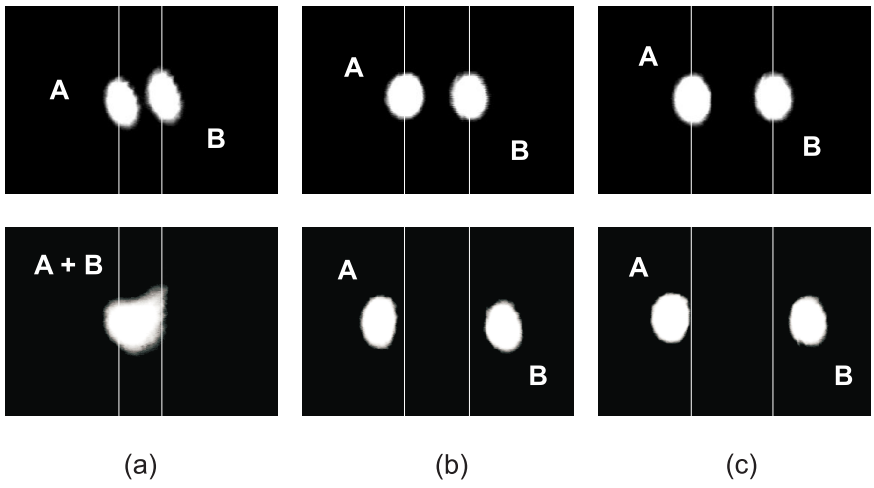

Fig. 8a–c. Experimental observation of separation-dependent interaction of incoherent solitons. The *x* axis is horizontal. **a** Fusion for close separation. **b**,**c** Repulsion of well-separated solitons

solitons. While this certainly is the case in isotropic self-focusing Kerr-type materials, the situation with PR media is, as we just showed above, more complex. Two incoherent solitons may experience both attractive and repulsive forces, depending on their relative separation and location in the crystal. As a consequence, there exist domains of attraction and repulsion in the transverse plane, which lead to the nontrivial topology of soliton trajectories when the beams are launched slanted to the direction of external field [39, 40]. A pair of solitons launched in a plane tilted at some angle with respect to the direction of applied field will initially rotate trying to align along the *y* axis, as this is the direction of strongest attraction. The momentum acquired by solitons produces an overshoot and, as the beams cross the *y* axis, the anisotropy of screening slows down the rate of rotation and reverses its direction. The distance between solitons decreases and the pair twists and turn about the *z* axis in a damped motion. When viewed along the *z* axis the motion initially resembles spiraling followed by oscillations predominantly along the *y* direction. The whole process ends with the soliton fusion. The distance where the beams fuse might be much larger than the typical thickness of the crystal. If the beams are launched anywhere outside the region of attraction, they repel and fly apart. We stress the fact that these trajectories are the result of the interaction of solitons that are initially coplanar. Such behaviour does not occur in a typical self-focusing material and is unique to the PR nonlinearity.

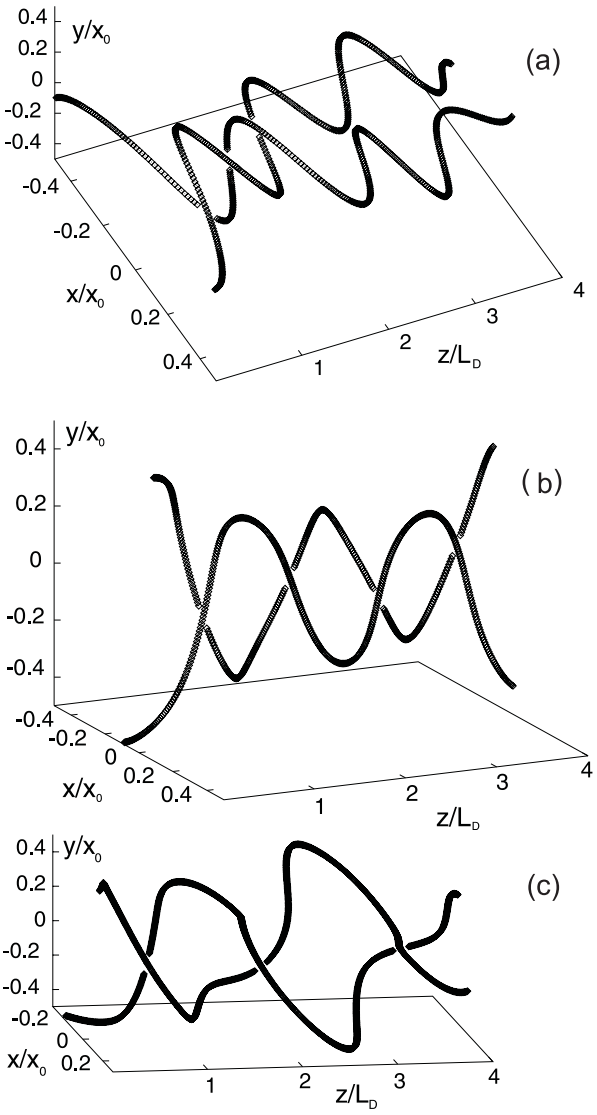

Fig. 10a–c. 3D trajectories of interacting incoherent solitons. **a** Rotating solitons. **b** Oscillating solitons. **c** Spiraling solitons

Generic examples of the motion of soliton pairs launched obliquely to the direction of the external field are shown in Fig. 10. The pairs shown in graphs Fig. 10a,b propagate initially in the same plane, whereas the initial conditions for the pair in Fig. 10c are slightly changed, to display prolonged spiraling. It is launched with a small tilt ($\theta_x = \mp 0.55$, $\theta_y = \mp 0.05$) and at a higher intensity ($|A|^2 = |B|^2 = 5.2$). The pair, shown in Fig. 10a, starts to rotate, however after one twist the beams partially unwind and remain on the same side of each other, producing damped oscillations. The pair in Fig. 10b performs elongated oscillations around the *y* axis from the beginning, wobbling along the way. The pair in Fig. 10c spirals for the whole length, with a swing about the *y* axis each time it is crossed.

The launching of skewed beams at a higher intensity offers the possibility of prolonged spiraling. Tilted beams carry initial angular momentum relative to the origin. However, the trajectory observed is not a simple, smooth spiral. The beams oscillate while spiraling. The "potential" in which the solitons rotate is not central. The long attractive well along the *y* axis always breaks the symmetry and prevents indefinite spiraling. In the end the solitons either fuse or fly apart. It should be mentioned that when the solitons are close to each other and interact strongly, they entangle and their individual identities are rather dubious. The light intensity distributions do not show two distinct beams anymore. However, as soon as the beams disentangle, two bright spots reappear.

The interaction of a pair of mutually incoherent spatial solitons with initially skewed trajectories was also investigated experimentally. Experimental evidence of the attraction-induced spiraling is presented in Fig. 11. Figure 11a shows both beams at the input face of the crystal, while Fig. 11b displays output position of the noninteracting solitons. Figure 11c shows the result of soliton interaction. It is clear that attraction of solitons resulted in mutual rotation of their trajectories. In this particular instance the rotation is $\approx 270^\circ$ over 13.5 mm distance.

5 Conclusions

In conclusion, we have discussed the interaction of incoherent soliton beams propagating in a PR medium. We have shown that spatial solitons in PR media exhibit anomalous interaction properties not seen in isotropic nonlinear media. In particular, while closely overlapping incoherent solitons always attract each other, larger separations may result in repulsive forces, depending on the size of separation and its orientation. This effect is a result of the nonlocal character of the anisotropic self-focusing in PR media, which leads to an effective self-defocusing in parts of the outer regions of the optical beam. This anisotropy of PR nonlinearity has profound consequences on the 3D soliton interaction. Whereas beams interacting in the plane perpendicular to the direction of applied electric field exhibit behaviour typical of sat-

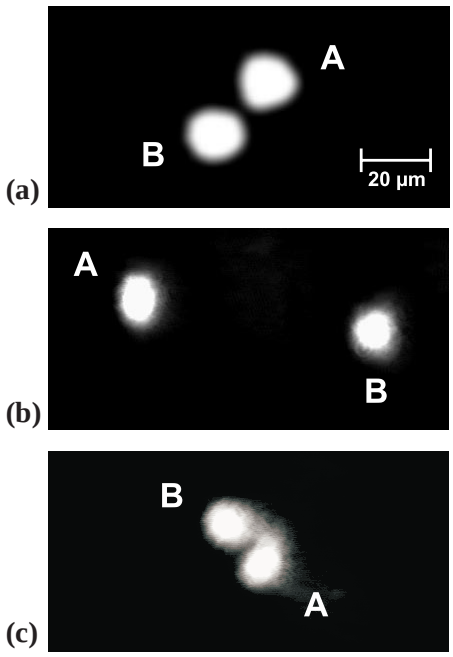

Fig. 11a–c. Experimentally observed attraction-induced soliton spiraling. **a** Input beams. **b** Non-interacting solitons. **c** Interacting solitons

urable self-focusing nonlinearity, featuring strong attraction and intersection for even initially diverging trajectories, those located in the plane along the direction of the field exhibit more complicated behaviour. Closely placed initially parallel solitons strongly attract, collide, and finally fuse, whereas well-separated beams repel. The off-axes launching leads to spirling motion even in the absence of any tangential velocity. Finally, the off-axes launching in combination with the initial angular tilt makes possible prolonged spiraling and oscillatory interaction behaviour. The beams perform complicated motion in the transverse plane, rotating about the origin, twisting and turning in the region of attraction. Eventually, they fuse. We find that the interaction between incoherent screening solitons is basically anisotropic, which may not be apparent in the early stages of soliton propagation. Close correspondence between experiments and the predictions of a three-dimensional model is obtained.

Acknowledgements. W. K. acknowledges support of the Alexander von Humboldt Stiftung. Darmstadt researchers are indebted to Prof. Dr. T. Tschudi and Prof. Dr. F. Kaiser for support and helpful discussions.

References

1. M.D. Iturbe-Castillo, P.A. Marquez-Aguilar, J.J. Sanchez-Mondragon, S. Stepanov, V. Vysloukh: Appl. Phys. Lett. **64**, 408 (1994)
2. M. Segev, G.C. Valley, B. Crosignani, P. DiPorto, A. Yariv: Phys. Rev. Lett. **73**, 3211 (1994)
3. D.N. Christodoulides, M.I. Carvalho: J. Opt. Soc. Am. B **12**, 1628 (1995)
4. M. Shih, M. Segev, G.C. Valley, G. Salamo, B. Crosignani, P. DiPorto: Electron. Lett. **31**, 826 (1995)
5. Z. Sheng, Y. Cui, Y. Cheng, Y. Wei: J. Opt. Soc. Am. B **13**, 584 (1996)
6. A.A. Zozulya, D.Z. Anderson: Phys. Rev. A **51**, 1520 (1995)
7. A.A. Zozulya, A.V. Mamaev, M. Saffman, D.Z. Anderson: Europhys. Lett. **36**, 419 (1996); A.A. Zozulya, A.V. Mamaev, M. Saffman, D. Anderson: Phys. Rev. A **54**, 870 (1996)
8. T. Shi, S. Chi: Opt. Lett. **15**, 1123 (1990); A.W. Snyder, D.J. Mitchell, L. Poladian, F. Ladouceur: Opt. Lett. **16**, 21 (1991); R. McLeod, K. Wagner, S. Blair: Phys. Rev. A **52**, 3254 (1995); P.D. Miller, N.N. Akhmediev: Phys. Rev. E **53**, 4098 (1996)
9. W.J. Firth, A.J. Scroggie: Phys. Rev. Lett. **76**, 1623 (1996); M. Brambilla, L.A. Lugiato, M. Stefani: Europhys. Lett. **34**, 109 (1996)
10. B. Luther-Davies, X. Yang: Opt. Lett. **17**, 498 (1992); B. Luther-Davies, X. Yang, W. Królikowski: Int. J. Nonlin. Opt. Mater. **2**, 339 (1993)
11. R. de la Fuente, A. Barthelemy, C. Froehly: Opt. Lett. **16**, 793 (1991)
12. G.S. Garćia-Quirino et al.: Opt. Lett. **22**, 154 (1997)
13. H. Meng, G. Salamo, M.F. Shih, M. Segev: Opt. Lett. **22**, 448 (1997)
14. A.V. Mamaev, M. Saffman, A.A. Zozulya: J. Opt. Soc. Am. B **15**, 2079 (1998)
15. W. Królikowski, S.A. Holmstrom: Opt. Lett. **22**, 369 (1997)
16. W. Królikowski, B. Luther-Davis, C. Denz, T. Tschudi: Opt. Lett. **23**, 97 (1998)
17. M.F. Shih et al.: Appl. Phys. Lett. **69**, 4151 (1996); M.F. Shih, M. Segev: Opt. Lett. **21**, 1538 (1996)
18. M. Shih, M. Segev, G. Salamo: Phys. Rev. Lett. **78**, 2551 (1997)
19. A.V. Buryak, Y.S. Kivshar, M. Shih, M. Segev: Phys. Rev. Lett. **82**, 81 (1999)
20. Degree of saturation determines not only the steady-state parameters of the screening solitons, but more importantly the rate of convergence of input beams to a soliton solution. For moderate saturation ($I \approx 1$) this convergence is fast enough for the solitons to be observed under typical experimental conditions. On the other hand, for strong saturation convergence is much weaker, so an initial Gaussian beam exhibits long transients before evolving into a soliton [7, 23]
21. M. Saffman, A.A. Zozulya: Opt. Lett. **23**, 1579 (1998)
22. J.H. Marburger: Prog. Quantum Electron. **4**, 35 (1975)
23. A.A. Zozulya, D.Z. Anderson, A.V. Mamaev, M. Saffman: Phys. Rev. A **57**, 622 (1998)
24. S. Gatz, J. Herrmann: Opt. Lett. **23**, 1176 (1998)
25. N.V. Kukhtarev et al.: Ferroelectrics **22**, 949 (1979)
26. A. Stepken, F. Kaiser, M. Belić, W. Królikowski: Phys. Rev. E **58**, R4112 (1998)
27. R.R. Neurgaonkar, W.K. Cory: J. Opt. Soc. Am. B **3**, 274 (1986)
28. P. Günter, J.P. Huignard (Eds.): *Photorefractive Materials and their Applications I* (Springer, Berlin, Heidelberg 1991)
29. M.I. Carvalho, S.R. Singh, D.N. Christodoulides: Opt. Commun. **120**, 311 (1995)
30. W. Królikowski, N. Akhmediev, B. Luther-Davies, M. Cronin-Golomb: Phys. Rev. E **54**, 5761 (1996)
31. W. Królikowski, M. Saffman, B. Luther-Davies, C. Denz: Phys. Rev. Lett. **80**, 3240 (1998)
32. N. Korneev et al.: J. Mod. Opt. **43**, 311 (1996)
33. C.M. Gomez Sarabia, P.A. Marquez Aguilar, J.J. Sanchez Mondragon, S. Stepanov, V. Vysloukh: J. Opt. Soc. Am. B **13**, 2767 (1996)
34. L. Poladian, A.W. Snyder, D.J. Mitchell: Opt. Commun. **85**, 59 (1991); D.J. Mitchell, A.W. Snyder, L. Poladian: Phys. Rev. Lett. **77**, 271 (1996)
35. V.E. Zakharov, A.B. Shabat: Sov. Phys. JETP **34**, 62 (1972)
36. J. Oficjalski, I. Białynicki-Birula: Acta Phys. Pol. B **9**, 759 (1978)
37. S. Cowan, R.H. Enns, S.S. Rangnekar, S. Sanghera: Can. J. Phys. **64**, 311 (1986); S. Gatz, J. Herrmann: Opt. Lett. **17**, 484 (1992)
38. A.W. Snyder, A.P. Sheppard: Opt. Lett. **18**, 482 (1993)
39. A. Stepken, M. Belic, F. Kaiser, W. Królikowski, B. Luther-Davies: Phys. Rev. Lett. **82**, 540 (1999)
40. M. Belic, A. Stepken, F. Kaiser: Phys. Rev. Lett. **82**, 544 (1999)